

## The antiviral compound remdesivir potently inhibits RNA-dependent RNA polymerase from Middle East respiratory syndrome coronavirus

Calvin J. Gordon<sup>1#</sup>, Egor P. Tchesnokov<sup>1#</sup>, Joy Y. Feng<sup>3</sup>, Danielle P. Porter<sup>3</sup> and Matthias Götze<sup>1,2\*</sup>

From the <sup>1</sup> Department of Medical Microbiology and Immunology, University of Alberta, Edmonton, Alberta, Canada; <sup>2</sup> Li Ka Shing Institute of Virology at University of Alberta, Edmonton, Alberta, Canada; <sup>3</sup> Gilead Sciences, Inc., Foster City, California, USA

### Running title:

Coronavirus Polymerase Inhibition with Remdesivir

\* To whom correspondence should be addressed: Matthias Götze: Department of Medical Microbiology and Immunology, University of Alberta, Edmonton, Alberta, Canada, T6G 2E1; [gotte@ualberta.ca](mailto:gotte@ualberta.ca); Tel.1(780) 492-2308.

# CJG and EPT contributed equally to this work.

**Keywords:** coronavirus, Middle East respiratory syndrome coronavirus (MERS-CoV), Severe Acute Respiratory Syndrome coronavirus 2 (SARS-CoV-2), Ebola virus (EBOV), RNA-dependent RNA polymerase (RdRp), remdesivir, positive-sense RNA virus, antiviral drug, RNA chain termination, viral replicase

### ABSTRACT

Antiviral drugs for managing infections with human coronaviruses are not yet approved, posing a serious challenge to current global efforts aimed at containing the outbreak of severe acute respiratory syndrome coronavirus 2 (SARS-CoV-2). Remdesivir (RDV) is an investigational compound with a broad spectrum of antiviral activities against RNA viruses, including SARS-CoV and Middle East respiratory syndrome (MERS-CoV). RDV is a nucleotide analog inhibitor of RNA-dependent RNA polymerases (RdRps). Here, we co-expressed the MERS-CoV nonstructural proteins nsp5, nsp7, nsp8, and nsp12 (RdRp) in insect cells as a part a polyprotein to study the mechanism of inhibition of MERS-CoV RdRp by RDV. We initially demonstrated that nsp8 and nsp12 form an active complex. The triphosphate form of the inhibitor (RDV-TP) competes with its natural counterpart ATP. Of note, the selectivity value for RDV-TP obtained here with a steady-state approach suggests that it is more efficiently incorporated than ATP and two other nucleotide analogues. Once incorporated at position i, the inhibitor caused RNA synthesis arrest at position i+3. Hence,

the likely mechanism of action is delayed RNA chain termination. The additional three nucleotides may protect the inhibitor from excision by the viral 3'-5' exonuclease activity. Together, these results help to explain the high potency of RDV against RNA viruses in cell-based assays.

The emergence of a novel coronavirus, named Severe Acute Respiratory Syndrome coronavirus 2 (SARS-CoV-2, formerly 2019-nCoV), initiated a global effort to identify effective treatments focusing on agents with demonstrated antiviral activity against SARS-CoV, Middle East respiratory syndrome (MERS-CoV) or related positive-sense RNA viruses. Although currently there are no approved antiviral drugs for the treatment of human coronavirus infections available, preclinical data with the nucleotide analogue Remdesivir (RDV) are promising and human safety data are available (1). This compound shows a broad spectrum of antiviral activities against several RNA viruses (2-4), including SARS-CoV and MERS-CoV (5). RDV was originally developed for the treatment of Ebola virus disease (EVD) (2). Cell-culture and animal studies revealed potent antiviral activities

against Filoviruses, including the Ebola virus (EBOV) (4). Subsequent studies have shown that RDV is also active against coronaviruses with divergent RNA-dependent RNA polymerases (RdRp) (5,6). However, biochemical data that support these findings and provide a possible mechanism of action are not available.

The triphosphate form of RDV (RDV-TP) was shown to inhibit the RdRp of Respiratory Syncytial Virus (RSV) (4), Nipah virus and Ebola Virus (EBOV) (7,8), which are all non-segmented negative-sense RNA viruses. Active Ebola RdRp contains the viral L protein in complex with viral protein 35 (VP35) (9,10). VP35 is the functional counterpart of the P protein of RSV and Nipah (7,11,12). Previously, we generated recombinant Ebola RdRp for the study of nucleotide analogue inhibitors (8). Enzyme kinetics show that RDV-TP is able to compete with its natural counterpart ATP for incorporation. The selectivity of ATP over the inhibitor is ~ 4-fold. Once incorporated at position *i*, the compound causes inhibition of RNA synthesis predominantly at position *i*+5. Delayed chain-termination is therefore a plausible mechanism of action.

Progress has also been made in characterizing the SARS-CoV RdRp complex (13-15). Biochemical data suggest that the active complex is composed of at least three viral non-structural proteins nsp7, nsp8 and nsp12. The RNA polymerase nsp12 alone displays low processivity. Synthesis of longer reaction products require the additional presence of nsp7 and nsp8. Although a heterotrimer was not stable, nsp7 and nsp8 can be linked together to form a complex with nsp12 (15). Here we developed a novel expression system for the MERS-CoV RdRp complex and studied the mechanism of action of remdesivir. Co-expression of the MERS nsp5 protease with nsp7, nsp8 and nsp12 in insect cells yielded a stable complex composed of nsp8 and nsp12. We demonstrate that this complex is active on model primer/template substrates that adequately mimic the elongation state. Most importantly, selectivity measurements determined here under the inherent limitations of the steady-state conditions revealed that incorporation of the inhibitor is more efficient

than its natural counterpart and delayed chain-termination is observed at position *i*+3.

## Results

### *Expression of MERS-CoV RdRp complex*

The Baculovirus expression system has recently been used to produce recombinant nsp12 from SARS-CoV (13). For SARS-CoV, an active RdRp complex was reconstituted with purified nsp7 and nsp8, with and without a linker, expressed in *Escherichia coli* (*E.coli*) (13,15). Here, we employed an alternative approach whereby MERS nsp5, nsp7, nsp8 and nsp12 were co-expressed in insect cells as a part a polyprotein (NCBI: YP\_009047202.1). The polyprotein was post-translationally cleaved by the nsp5 protease at its original cleavage sites (Fig. 1A). We also expressed a MERS-CoV RdRp complex in which the catalytic residues within the conserved motif C (SDD) of nsp12 were mutated (SNN) to generate an inactive RdRp (Fig. 1B) (16).

Ni-NTA affinity chromatography via the N-terminal eight-histidine tag of the nsp8 protein resulted in a MERS-CoV RdRp complex containing nsp8 (~23 kDa) and nsp12 (~110 kDa) (Fig. 1C). Mass spectroscopy confirmed the presence of nsp8 and nsp12, while there was no evidence for the presence of nsp7.

The wild type MERS-CoV RdRp complex was tested for RNA synthesis on short model primer/template substrates mimicking a random elongation complex during RNA synthesis. We recently used the same model substrates for the study of other RdRp enzymes (Fig. 1D) (8,10). The 4nt-primer/14-mer templates are designed such that [ $\alpha$ -<sup>32</sup>P]GTP is the first incorporated nucleotide, which labels the RNA products. Reactions containing the MERS-CoV RdRp complex, primer/template and various combinations of NTPs were initiated by the addition of Mg<sup>2+</sup> ions. In the presence [ $\alpha$ -<sup>32</sup>P]GTP alone the expected 5-mer product is formed. Addition of specific combinations of NTPs generated defined reaction products - [ $\alpha$ -<sup>32</sup>P]GTP and ATP yielded a 7-mer (Fig. 1D, left side of the gel) or a 6-mer product (Fig. 1D, right side of the gel), depending on the template sequence. Similarly, in the presence of [ $\alpha$ -<sup>32</sup>P]GTP, ATP and CTP (or UTP) the 4-mer primer is extended to yield an 11-mer or a 7-mer depending on the

template sequence. Addition of all four NTPs resulted in a 14-mer full-length product. Reactions with the SNN mutant enzyme did not show RNA product formation. The lane “[ $\alpha$ - $^{32}$ P]GTP only” illustrates the background signal associated with the [ $\alpha$ - $^{32}$ P]GTP preparation in the absence of enzyme. This data confirms that MERS-CoV nsp12 exhibits the observed RdRp activity. It has recently reported that SARS-CoV nsp8 displays RNA primase activity that yields short (~ 6-mer) reaction products (15,17). However, structural data are inconsistent with the formation of a primase active site in SARS-CoV nsp8 (13), and our data do not provide any evidence for primase activity in MERS-CoV nsp8.

### ***Inhibition of EBOV RdRp and MERS-CoV RdRp with RDV***

For EBOV RdRp, it has been challenging to identify a sequence with a single site of incorporation for the RDV. Hence, we devised two different RNA templates that allow multiple and single incorporations, respectively, as shown in Figure 1A. These sequences were used to compare the inhibitory effects of RDV on EBOV RdRp and MERS RdRp. For EBOV RdRp, we observed delayed chain-termination at position i+5 as previously described (Fig. 2B) (8). However, the template that provides a single site of RDV-TP incorporation also shows reductions in full-length RNA synthesis. In contrast, the MERS RdRp complex yields the full-length RNA product with both sequences. The inhibition patterns with RDV-TP differ markedly from our results with EBOV RdRp. RNA synthesis is arrested at positions i+3 and i+4 with a template that provides multiple sites of incorporation of the inhibitor and the full-length product is only seen as a faint band. The template that allows only a single incorporation event yields RNA synthesis arrest at position i+3 and an increased amount of the full-length product. Hence, the mechanism of inhibition is likely delayed chain-termination for both EBOV RdRp and MERS RdRp although the specific patterns show subtle differences. In the absence of inhibitor, RNA synthesis and full-length product formation is generally more efficient with MERS-CoV RdRp. This could also help to explain that a small amount of full-length product is still seen with this enzyme in the presence of inhibitor.

### ***Competitive inhibition of RNA synthesis by RDV-TP.***

To study whether RDV-TP is able to compete with its natural counterpart ATP we monitored RNA synthesis at a fixed concentration of NTPs (0.02  $\mu$ M) and increasing concentrations of RDV-TP (Fig. 3A, top). Increasing concentrations of RDV-TP caused a reduction of the 14-mer product due to increases in RNA synthesis arrest at position i+3. Formation of the full-length 14-mer product is not evident at RDV-TP concentrations higher than 0.041  $\mu$ M. Quantification of the data revealed an  $IC_{50}$  for RDV-TP of 0.032  $\mu$ M under these conditions (Fig. 3B). This value is only 1.5-fold higher than the ATP concentration, which points to an efficient use of the inhibitor. Increasing concentrations of ATP caused a corresponding increase in  $IC_{50}$  values for RDV-TP (Fig. 3C), which shows that RDV-TP is a competitive inhibitor.

### ***Selectivity measurements of ATP-analogues.***

To translate our previous findings into quantitative terms we determined Michaelis-Menten parameters  $V_{max}$  and  $K_m$ , and calculated the efficiency  $V_{max}/K_m$  of nucleotide incorporation for ATP, RDV-TP and two other nucleotide analogue inhibitors for comparative purpose: ara-ATP and 2'CM-ATP (Fig. 4). ATP, or the ATP analogue, was added at increasing concentrations and the reactions were stopped after 20 minutes following the addition of  $Mg^{2+}$ . This approach allowed us to determine the selectivity for nucleotide incorporation, defined as  $V_{max}/K_m$  (ATP) over  $V_{max}/K_m$  (nucleotide analogue) (Table 1). The observed differences in the efficiencies of nucleotide analogue substrate utilization are driven solely by differences in the respective  $K_m$  values. The data show an unexpectedly low selectivity value for RDV-TP (0.35), while ara-ATP (749) and 2'CM-ATP (165) are both associated with high selectivity values. The selectivity value for RDV-TP below 1 suggests that incorporation of the inhibitor is more efficient as compared to the natural substrate. Commonly, the nucleotide analogue is less efficiently incorporated as seen with ara-ATP and 2'CM-ATP.

## Discussion

Broad spectrum antivirals or compounds with demonstrated activity against SARS-CoV or MERS-CoV are now considered for the treatment of infection caused by the novel coronavirus SARS-CoV-2. The nucleotide analogue RDV has been tested in a randomized, controlled trial for EVD (18). Although two other investigational therapies were more efficacious than RDV, an antiviral effect has been demonstrated. This compound also shows a broad spectrum of antiviral activities against coronaviruses *in vitro* and in animal models (1,6,19,20). Moreover, screening of a compound library of FDA-approved drugs revealed that the human immunodeficiency virus type 1 (HIV-1) protease inhibitor lopinavir (LPV) is active against MERS-CoV (21). This drug is currently tested in a clinical trial for the treatment of MERS-CoV in combination with interferon- $\beta$  (IFN $\beta$ ) and ritonavir (RTV) (22), which is used for pharmacological boosting. A recent study compared the efficacy of the combination of LPV/RTV/IFN $\beta$  with RDV in cell culture and showed that RDV was significantly more active against MERS-CoV (1). Here we focused on the biochemical evaluation of RDV to provide a better understanding of its broad spectrum of antiviral activities and the underlying mechanism of action.

*In vitro* selection experiments with the coronavirus model murine hepatitis virus (MHV) (5) resulted in two variants with resistance-conferring mutations in nsp12. This data provides strong evidence to show that RdRp is the target for RDV. Our biochemical data corroborate that the RNA polymerase of MERS-CoV is indeed the drug target. We demonstrate that MERS nsp8 and nsp12 form an active, binary complex. RDV-TP is utilized as a substrate and competes with its natural counterpart ATP. Natural nucleotide pools are commonly more efficiently incorporated when compared with nucleotide analogues. However, in this case, we observe that incorporation of the nucleotide analogue is significantly more efficient.

Once added into the growing RNA chain, the inhibitor does not cause immediate chain-termination. The presence of the 3'-hydroxyl group allows the addition of three more nucleotides until RNA synthesis is arrested at

position  $i+3$ . A fraction of the extended primer overcomes this arrest, which can lead to full-length product formation. Full-length product formation is considerably reduced when the inhibitor is added at consecutive sites. The efficient rate of RDV-TP incorporation may translate in multiple incorporation events *in vivo* and this could add to the overall potency of the drug. It is important to note that other parameters including the intracellular concentration of the triphosphate form of the inhibitor need to be considered as well.

The different inhibition patterns observed with EBOV RdRp and MERS-CoV RdRp point to subtle differences in the mechanism of action. Delayed chain-termination could be based on inhibitor-induced structural changes of the newly synthesized double-stranded RNA that at some point prevent a productive alignment of primer and incoming nucleotide, e.g. through primer/template repositioning (23), or backtracking mechanisms (24). Enzyme-specific interactions with the extended primer may likewise affect the continued extension of the primer, which helps to explain variations in the site of RNA synthesis arrest.

An open question that warrants further investigation is the role of the 3'-5' exonuclease (nsp14) in susceptibility to RDV. It has previously been reported that nucleotide analogue inhibitors can be excised by the viral exonuclease (14). An MHV mutant lacking the 3'-5' exonuclease activity was shown to be more sensitive to RDV (5). However, given its high potency in cell-based assays, RDV seems to be protected from excision at least to a certain degree. This protection could be provided by the additional three nucleotide following the inhibitor. In contrast, classic chain-terminators would be readily accessible for excision. Taken together, this study provides a likely mechanism of action for RDV against coronaviruses. The novel strategy for the expression of MERS-CoV RdRp helps to guide the design of equivalent constructs of related viruses, including SARS-CoV-2.



## Experimental procedures

### *Chemicals*

All RNA primers and templates used in this study were 5'-phosphorylated and purchased from Dharmacon (Lafayette, CO, USA). 2'-methyl-ATP (2'CM-ATP) and remdesivir-TP (RDV-TP) were by Gilead Sciences (Foster City, CA, USA). Ara-ATP was purchased from TriLink (San Diego, CA, USA). NTPs were purchased from GE Healthcare (Cranbury, NJ, USA). [ $\alpha$ - $^{32}$ P]-GTP was purchased from PerkinElmer (Boston, MA, USA).

### *Protein expression and purification*

The pFastBac-1 (Invitrogen, Burlington, ON, Canada) plasmid with the codon-optimized synthetic DNA sequences (GenScript, Piscataway, NJ, USA) coding for a portion of MERS-CoV lab polyprotein (NCBI: YP\_009047202.1) containing only nsp5, nsp7, nsp8 and nsp12 was used as a starting material for protein expression in insect cells (Sf9, Invitrogen, Burlington, ON, Canada). We employed the MultiBac (Geneva Biotech, Indianapolis, IN, USA) system for protein expression in insect cells (Sf9, Invitrogen, Burlington, ON, Canada) according to published protocols (25,26). MERS-CoV protein complex was purified using Ni-NTA affinity chromatography of the nsp8 N-terminal eight-histidine tag according to the manufacturer's specifications (Thermo Scientific, Rockford, IL, USA). The identities of the purified MERS-CoV proteins were confirmed by mass spectrometry (MS) analysis (Dr. Jack Moore, Alberta Proteomics and Mass Spectrometry, Edmonton, AB, Canada). Expression and purification of EBOV RdRp complex were performed as previously described (10).

### *RNA synthesis activity*

Data acquisition and quantification were done as previously reported by us (8,10). RNA synthesis assay consisted of mixing (final concentrations) Tris-HCl (pH 8, 25 mM), RNA primer (200  $\mu$ M), RNA template (1  $\mu$ M), [ $\alpha$ - $^{32}$ P]-NTP (0.1  $\mu$ M), various concentrations and combinations of 100  $\mu$ M (or as indicated) NTP and NTP analogues, and MERS-CoV RdRp

complex ( $\sim$ 0.1  $\mu$ M) on ice. Reaction mixtures (10  $\mu$ L) were incubated for 10 min at 30  $^{\circ}$ C followed by the addition of 5  $\mu$ L of MgCl<sub>2</sub> (2.5 mM). Reactions were stopped after 30 min by the addition of 15  $\mu$ L of formamide/EDTA (50 mM) mixture and incubated at 95  $^{\circ}$ C for 10 min. 3  $\mu$ L reaction samples were subjected to denaturing 8 M urea 20% polyacrylamide gel electrophoresis to resolve products of RNA synthesis followed by signal quantification (ImageQuant 5.2, GE Healthcare Bio-Sciences, Uppsala, Sweden) through phosphorimaging (Typhoon TRIO variable mode imager, GE Healthcare Bio-Sciences, Uppsala, Sweden). For nucleotide incorporation experiments, ATP or the ATP analogue inhibitor was added at increasing concentrations and the reactions were stopped at a fixed time point of 20 minutes following the addition of Mg<sup>2+</sup>. The reaction conditions were chosen such that the formation of the G5 product, i.e. the 4-mer primer extended with [ $\alpha$ - $^{32}$ P]GTP, was linear with respect to time at the 20 minute time point. The product fraction was determined from the total signal in G5 and i6 bands, plotted versus ATP or ATP analogue substrate concentrations and fitted to the Michaelis-Menten equation using GraphPad Prism 7.0 (GraphPad Software, Inc., San Diego, CA, USA) with  $V_{\max}$  and  $K_m$  parameters. Our assay involves incorporation of [ $\alpha$ - $^{32}$ P]GTP into the primer. With this approach it is not possible to quantify the fraction of the extended primer; however, the reaction products are clearly defined by the correct incorporation of [ $\alpha$ - $^{32}$ P]GTP. Potentially confounding byproducts due to misaligned primers are invisible. In case of IC<sub>50</sub> experiments the full template-length product fractions were plotted versus RDV-TP concentrations and fitted to a log(inhibitor)-versus-normalized-response-(variable slope) equation using GraphPad Prism 7.0 (GraphPad Software, Inc., San Diego, CA, USA) to determine the IC<sub>50</sub> values for the inhibition of RNA synthesis by RDV-TP. The concentrations of nucleotide substrate (0.02; 0.06; 0.12 and 0.24  $\mu$ M) in the competition assays were chosen around the  $K_m$  value for ATP (0.02  $\mu$ M, Table 1).

**Acknowledgements:** We would like to thank Emma Woolner for excellent technical assistance and Dr. Jack Moore at the Alberta Proteomics and Mass Spectrometry facility for mass spectrometry analysis.

**Conflict of interest:** MG has previously received funding from Gilead Sciences in support for the study of EBOV RdRp inhibition by RDV.

## References

1. Sheahan, T. P., Sims, A. C., Leist, S. R., Schafer, A., Won, J., Brown, A. J., Montgomery, S. A., Hogg, A., Babusis, D., Clarke, M. O., Spahn, J. E., Bauer, L., Sellers, S., Porter, D., Feng, J. Y., Cihlar, T., Jordan, R., Denison, M. R., and Baric, R. S. (2020) Comparative therapeutic efficacy of remdesivir and combination lopinavir, ritonavir, and interferon beta against MERS-CoV. *Nature communications* **11**, 222
2. Siegel, D., Hui, H. C., Doerffler, E., Clarke, M. O., Chun, K., Zhang, L., Neville, S., Carra, E., Lew, W., Ross, B., Wang, Q., Wolfe, L., Jordan, R., Soloveva, V., Knox, J., Perry, J., Perron, M., Stray, K. M., Barauskas, O., Feng, J. Y., Xu, Y., Lee, G., Rheingold, A. L., Ray, A. S., Bannister, R., Strickley, R., Swaminathan, S., Lee, W. A., Bavari, S., Cihlar, T., Lo, M. K., Warren, T. K., and Mackman, R. L. (2017) Discovery and Synthesis of a Phosphoramidate Prodrug of a Pyrrolo[2,1-f][triazin-4-amino] Adenine C-Nucleoside (GS-5734) for the Treatment of Ebola and Emerging Viruses. *Journal of medicinal chemistry* **60**, 1648-1661
3. Lo, M. K., Jordan, R., Arvey, A., Sudhamsu, J., Shrivastava-Ranjan, P., Hotard, A. L., Flint, M., McMullan, L. K., Siegel, D., Clarke, M. O., Mackman, R. L., Hui, H. C., Perron, M., Ray, A. S., Cihlar, T., Nichol, S. T., and Spiropoulou, C. F. (2017) GS-5734 and its parent nucleoside analog inhibit Filo-, Pneumo-, and Paramyxoviruses. *Scientific reports* **7**, 43395
4. Warren, T. K., Jordan, R., Lo, M. K., Ray, A. S., Mackman, R. L., Soloveva, V., Siegel, D., Perron, M., Bannister, R., Hui, H. C., Larson, N., Strickley, R., Wells, J., Stuthman, K. S., Van Tongeren, S. A., Garza, N. L., Donnelly, G., Shurtleff, A. C., Retterer, C. J., Gharaibeh, D., Zamani, R., Kenny, T., Eaton, B. P., Grimes, E., Welch, L. S., Gomba, L., Wilhelmsen, C. L., Nichols, D. K., Nuss, J. E., Nagle, E. R., Kugelman, J. R., Palacios, G., Doerffler, E., Neville, S., Carra, E., Clarke, M. O., Zhang, L., Lew, W., Ross, B., Wang, Q., Chun, K., Wolfe, L., Babusis, D., Park, Y., Stray, K. M., Trancheva, I., Feng, J. Y., Barauskas, O., Xu, Y., Wong, P., Braun, M. R., Flint, M., McMullan, L. K., Chen, S. S., Fearn, R., Swaminathan, S., Mayers, D. L., Spiropoulou, C. F., Lee, W. A., Nichol, S. T., Cihlar, T., and Bavari, S. (2016) Therapeutic efficacy of the small molecule GS-5734 against Ebola virus in rhesus monkeys. *Nature* **531**, 381-385
5. Agostini, M. L., Andres, E. L., Sims, A. C., Graham, R. L., Sheahan, T. P., Lu, X., Smith, E. C., Case, J. B., Feng, J. Y., Jordan, R., Ray, A. S., Cihlar, T., Siegel, D., Mackman, R. L., Clarke, M. O., Baric, R. S., and Denison, M. R. (2018) Coronavirus Susceptibility to the Antiviral Remdesivir (GS-5734) Is Mediated by the Viral Polymerase and the Proofreading Exoribonuclease. *mBio* **9**
6. Brown, A. J., Won, J. J., Graham, R. L., Dinno, K. H., 3rd, Sims, A. C., Feng, J. Y., Cihlar, T., Denison, M. R., Baric, R. S., and Sheahan, T. P. (2019) Broad spectrum antiviral remdesivir inhibits human endemic and zoonotic deltacoronaviruses with a highly divergent RNA dependent RNA polymerase. *Antiviral research* **169**, 104541
7. Jordan, P. C., Liu, C., Raynaud, P., Lo, M. K., Spiropoulou, C. F., Symons, J. A., Beigelman, L., and Deval, J. (2018) Initiation, extension, and termination of RNA synthesis by a paramyxovirus polymerase. *PLoS pathogens* **14**, e1006889

8. Tchesnokov, E. P., Feng, J. Y., Porter, D. P., and Gotte, M. (2019) Mechanism of Inhibition of Ebola Virus RNA-Dependent RNA Polymerase by Remdesivir. *Viruses* **11**
9. Muhlberger, E., Weik, M., Volchkov, V. E., Klenk, H. D., and Becker, S. (1999) Comparison of the transcription and replication strategies of marburg virus and Ebola virus by using artificial replication systems. *Journal of virology* **73**, 2333-2342
10. Tchesnokov, E. P., Raeisimakiani, P., Ngure, M., Marchant, D., and Gotte, M. (2018) Recombinant RNA-Dependent RNA Polymerase Complex of Ebola Virus. *Scientific reports* **8**, 3970
11. Deval, J., Hong, J., Wang, G., Taylor, J., Smith, L. K., Fung, A., Stevens, S. K., Liu, H., Jin, Z., Dyatkina, N., Prhavic, M., Stoycheva, A. D., Serebryany, V., Liu, J., Smith, D. B., Tam, Y., Zhang, Q., Moore, M. L., Fearn, R., Chanda, S. M., Blatt, L. M., Symons, J. A., and Beigelman, L. (2015) Molecular Basis for the Selective Inhibition of Respiratory Syncytial Virus RNA Polymerase by 2'-Fluoro-4'-Chloromethyl-Cytidine Triphosphate. *PLoS pathogens* **11**
12. Noton, S. L., Deflube, L. R., Tremaglio, C. Z., and Fearn, R. (2012) The respiratory syncytial virus polymerase has multiple RNA synthesis activities at the promoter. *PLoS pathogens* **8**, e1002980
13. Kirchdoerfer, R. N., and Ward, A. B. (2019) Structure of the SARS-CoV nsp12 polymerase bound to nsp7 and nsp8 co-factors. *Nature communications* **10**, 2342
14. Ferron, F., Subissi, L., Silveira De Morais, A. T., Le, N. T. T., Sevajol, M., Gluais, L., Decroly, E., Vonrhein, C., Bricogne, G., Canard, B., and Imbert, I. (2017) Structural and molecular basis of mismatch correction and ribavirin excision from coronavirus RNA. *Proceedings of the National Academy of Sciences of the United States of America*
15. Subissi, L., Posthuma, C. C., Collet, A., Zevenhoven-Dobbe, J. C., Gorbalenya, A. E., Decroly, E., Snijder, E. J., Canard, B., and Imbert, I. (2014) One severe acute respiratory syndrome coronavirus protein complex integrates processive RNA polymerase and exonuclease activities. *Proceedings of the National Academy of Sciences of the United States of America* **111**, E3900-3909
16. Poch, O., Sauvaget, I., Delarue, M., and Tordo, N. (1989) Identification of four conserved motifs among the RNA-dependent polymerase encoding elements. *The EMBO journal* **8**, 3867-3874
17. Imbert, I., Guillemot, J. C., Bourhis, J. M., Bussetta, C., Coutard, B., Egloff, M. P., Ferron, F., Gorbalenya, A. E., and Canard, B. (2006) A second, non-canonical RNA-dependent RNA polymerase in SARS coronavirus. *The EMBO journal* **25**, 4933-4942
18. Mulangu, S., Dodd, L. E., Davey, R. T., Jr., Tshiani Mbaya, O., Proschan, M., Mukadi, D., Lusakibanza Manzo, M., Nzolo, D., Tshomba Oloma, A., Ibanda, A., Ali, R., Coulibaly, S., Levine, A. C., Grais, R., Diaz, J., Lane, H. C., Muyembe-Tamfum, J. J., Sivahera, B., Camara, M., Kojan, R., Walker, R., Dighero-Kemp, B., Cao, H., Mukumbayi, P., Mbala-Kingebeni, P., Ahuka, S., Albert, S., Bonnett, T., Crozier, I., Duvenhage, M., Proffitt, C., Teitelbaum, M., Moench, T., Aboulhab, J., Barrett, K., Cahill, K., Cone, K., Eckes, R., Hensley, L., Herpin, B., Higgs, E., Ledgerwood, J., Pierson, J., Smolskis, M., Sow, Y., Tierney, J., Sivapalasingam, S., Holman, W., Gettinger, N., Vallee, D., and Nordwall, J. (2019) A Randomized, Controlled Trial of Ebola Virus Disease Therapeutics. *The New England journal of medicine* **381**, 2293-2303
19. Sheahan, T. P., Sims, A. C., Graham, R. L., Menachery, V. D., Gralinski, L. E., Case, J. B., Leist, S. R., Pyrc, K., Feng, J. Y., Trantcheva, I., Bannister, R., Park, Y., Babusis, D.,

- Clarke, M. O., Mackman, R. L., Spahn, J. E., Palmiotti, C. A., Siegel, D., Ray, A. S., Cihlar, T., Jordan, R., Denison, M. R., and Baric, R. S. (2017) Broad-spectrum antiviral GS-5734 inhibits both epidemic and zoonotic coronaviruses. *Science translational medicine* **9**
20. de Wit, E., Feldmann, F., Cronin, J., Jordan, R., Okumura, A., Thomas, T., Scott, D., Cihlar, T., and Feldmann, H. (2020) Prophylactic and therapeutic remdesivir (GS-5734) treatment in the rhesus macaque model of MERS-CoV infection. *Proceedings of the National Academy of Sciences*, 201922083
  21. de Wilde, A. H., Jochmans, D., Posthuma, C. C., Zevenhoven-Dobbe, J. C., van Nieuwkoop, S., Bestebroer, T. M., van den Hoogen, B. G., Neyts, J., and Snijder, E. J. (2014) Screening of an FDA-approved compound library identifies four small-molecule inhibitors of Middle East respiratory syndrome coronavirus replication in cell culture. *Antimicrobial agents and chemotherapy* **58**, 4875-4884
  22. Arabi, Y. M., Asiri, A. Y., Assiri, A. M., Aziz Jokhdar, H. A., Alothman, A., Balkhy, H. H., AlJohani, S., Al Harbi, S., Kojan, S., Al Jeraisy, M., Deeb, A. M., Memish, Z. A., Ghazal, S., Al Faraj, S., Al-Hameed, F., AlSaedi, A., Mandourah, Y., Al Mekhlafi, G. A., Sherbeeni, N. M., Elzein, F. E., Almotairi, A., Al Bshabshe, A., Kharaba, A., Jose, J., Al Harthy, A., Al Sulaiman, M., Mady, A., Fowler, R. A., Hayden, F. G., Al-Dawood, A., Abdelzaher, M., Bajhmom, W., and Hussein, M. A. (2020) Treatment of Middle East respiratory syndrome with a combination of lopinavir/ritonavir and interferon-beta1b (MIRACLE trial): statistical analysis plan for a recursive two-stage group sequential randomized controlled trial. *Trials* **21**, 8
  23. Tchesnokov, E. P., Obikhod, A., Schinazi, R. F., and Gotte, M. (2008) Delayed chain termination protects the anti-hepatitis B virus drug entecavir from excision by HIV-1 reverse transcriptase. *The Journal of biological chemistry* **283**, 34218-34228
  24. Dulin, D., Arnold, J. J., van Laar, T., Oh, H. S., Lee, C., Perkins, A. L., Harki, D. A., Depken, M., Cameron, C. E., and Dekker, N. H. (2017) Signatures of Nucleotide Analog Incorporation by an RNA-Dependent RNA Polymerase Revealed Using High-Throughput Magnetic Tweezers. *Cell reports* **21**, 1063-1076
  25. Berger, I., Fitzgerald, D. J., and Richmond, T. J. (2004) Baculovirus expression system for heterologous multiprotein complexes. *Nature biotechnology* **22**, 1583-1587
  26. Bieniossek, C., Richmond, T. J., and Berger, I. (2008) MultiBac: multigene baculovirus-based eukaryotic protein complex production. *Current protocols in protein science / editorial board, John E. Coligan ... [et al.]* **Chapter 5**, Unit 5 20

## FOOTNOTES

This study was supported by grants to MG from the Canadian Institutes of Health Research (CIHR, grant number 159507) and from the Alberta Ministry of Economic Development, Trade and Tourism by the Major Innovation Fund Program for the AMR – One Health Consortium.

The abbreviations used are: RdRp, RNA-dependent RNA polymerase; remdesivir-TP, RDV-TP; 2'C-methyl-ATP, 2'CM-ATP.



**Table 1. MERS RdRp complex selectivity values for ATP analogues.**

	ATP	RDV-TP	ara-ATP	2'CM-ATP
	n = 7	n = 6	n = 5	n = 5
$V_{\max}^a$ (product fraction)	<b>0.47<sup>d</sup></b>	<b>0.50</b>	<b>0.48</b>	<b>0.47</b>
±	0.011 <sup>e</sup>	0.012	0.019	0.021
% error <sup>f</sup>	2	2	4	4
$K_m^b$ ( $\mu\text{M}$ )	<b>0.017</b>	<b>0.0063</b>	<b>13</b>	<b>2.8</b>
±	0.0019	0.00069	1.7	0.53
% error	11	11	13	19
$V_{\max}/K_m$	28	79	0.037	0.17
<b>Selectivity<sup>c</sup></b> (fold)	1 <sup>f</sup>	<b>0.35</b>	<b>749</b>	<b>165</b>

<sup>a</sup>  $V_{\max}$  is a Michaelis–Menten parameter reflecting the maximal velocity of nucleotide incorporation.

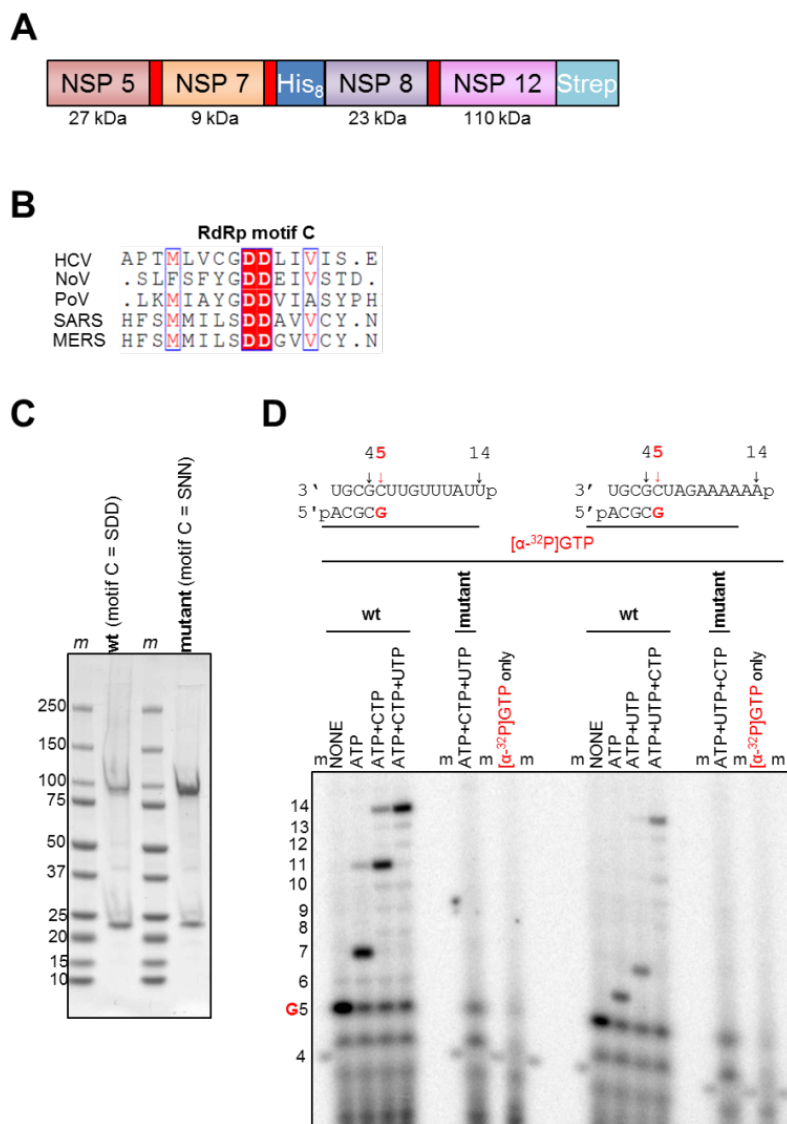
<sup>b</sup>  $K_m$  is a Michaelis–Menten parameter reflecting the concentration of the nucleotide substrate at which the velocity of nucleotide incorporation is half of  $V_{\max}$ .

<sup>c</sup> Selectivity of a viral RNA polymerase for a nucleotide substrate analogue is calculated as the ratio of the  $V_{\max}/K_m$  values for NTP and NTP analogue, respectively.

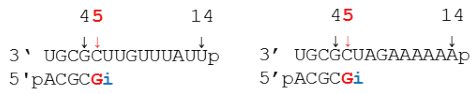
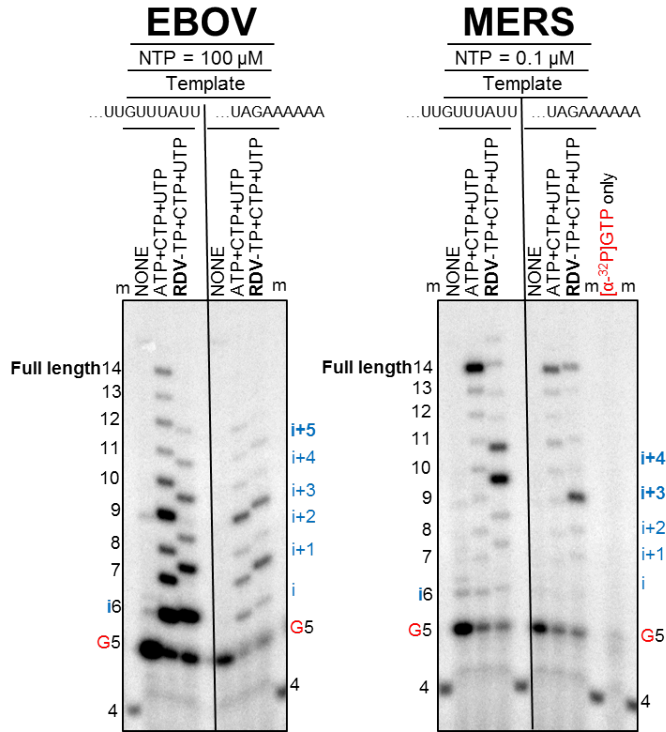
<sup>d</sup> All reported values have been calculated on the basis of a 9-data point experiment repeated indicated number of times (n).

<sup>e</sup> Standard error associated with the fit.

<sup>f</sup>Reference.



**Figure 1.** Expression, purification and characterization of the MERS RdRp complex. **(A)** The construct contains non-structural proteins nsp5, nsp7, nsp8 and nsp12. Red rectangles indicate original nsp5 protease cleavage sites. His<sub>8</sub> and Strep indicate the location of histidine- and strep- tags, respectively. **(B)** A snapshot of a sequence alignment (T-Coffee) of representative RdRp enzymes from positive-sense RNA genome viruses illustrating sequence conservation within RdRp motif C. **(C)** SDS PAGE migration pattern of the purified enzyme preparations stained with Coomassie Brilliant Blue G-250 dye. Proteins migrating at ~100 and ~25 kDa contain nsp12 and nsp8, respectively. **(D)** RNA synthesis on a short model primer/template substrate. Template and primer were both phosphorylated (p) at their 5'-ends. G indicates incorporation of the radiolabeled nucleotide opposite template position 5. RNA synthesis was monitored with the purified MERS RdRp complex wt (motif C = SDD) and active site mutant (motif C = SNN) in the presence of NTP combinations designed to generate specific products. Lane m illustrates the migration pattern of the radiolabeled 4 nucleotide-long primer.

**A****B**

**Figure 2.** Patterns of inhibition of RNA synthesis with remdesivir-TP (RDV-TP). **(A)** RNA primer/template substrates used to test multiple (left) or single (right) incorporations of RDV-TP. G indicates incorporation of the radiolabeled nucleotide opposite template position 5. i indicates incorporation site for the first (left) or the only (right) RDV-TP. Full length indicates the full-template length products of RNA synthesis. **(B)** RDV-TP incorporation was monitored with purified EBOV and MERS RdRp complexes in the presence of indicated combinations of NTPs and RDV-TP.

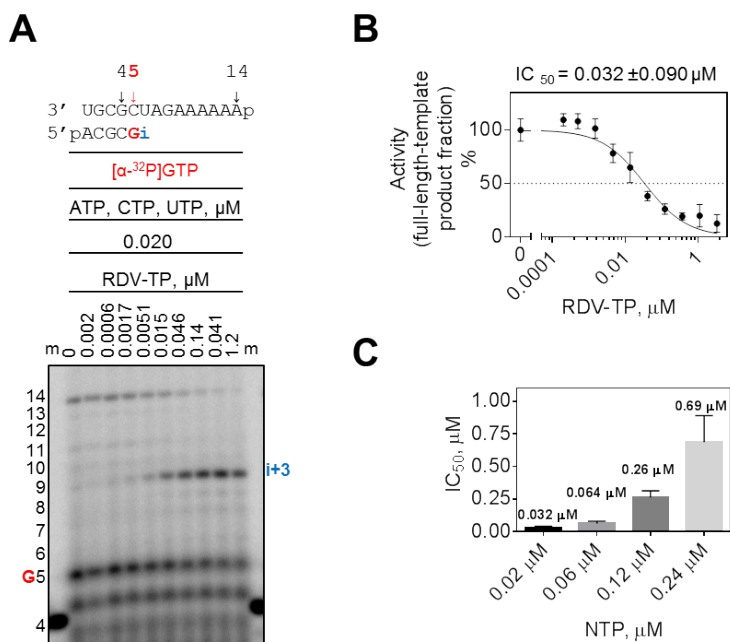


**Figure 3.** Competition between RDV-TP and ATP. **(A)** The RNA primer/template substrate used in this assay is shown above the gel. G indicates incorporation of the radiolabeled nucleotide opposite template position 5. Position i allows incorporation of ATP or RDV-TP. RNA synthesis was monitored with purified MERS RdRp complex in the presence of 0.02 μM ATP, CTP and UTP mix and increasing concentrations of RDV-TP as indicated. **(B)** Graphic representation and IC<sub>50</sub> determination fitting of quantified data from panel A. Error bars represent standard deviation of the data within four independent experiments. **(C)** Graphic representation of the relationship between IC<sub>50</sub> values for RDV-TP measured at different NTP concentrations. Average IC<sub>50</sub> values for RDV-TP are shown above the corresponding bars. Error bars represent standard deviation of the data within at least three independent experiments.



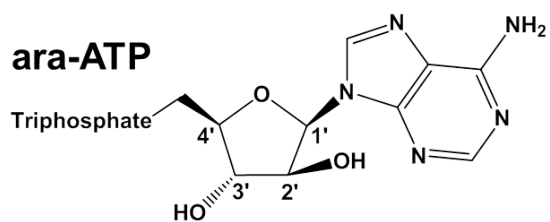
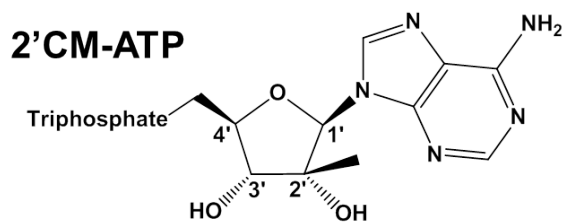
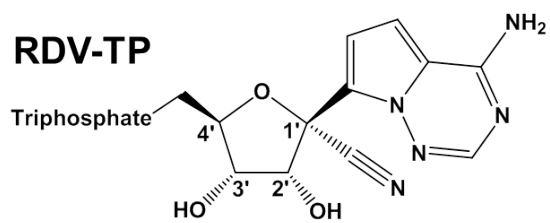
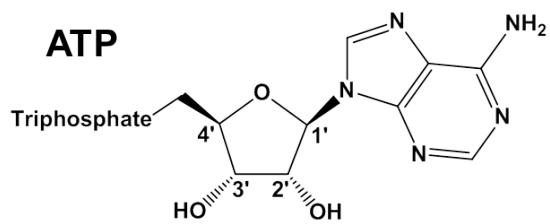


**Figure 4.** Chemical structures of ATP and ATP-analogues.

**The antiviral compound remdesivir potently inhibits RNA-dependent RNA polymerase from Middle East respiratory syndrome coronavirus**  
Calvin J Gordon, Egor P Tchesnokov, Joy Y. Feng, Danielle P Porter and Matthias Gotte  
*J. Biol. Chem.* published online February 24, 2020

---

Access the most updated version of this article at doi: [10.1074/jbc.AC120.013056](https://doi.org/10.1074/jbc.AC120.013056)

Alerts:

- [When this article is cited](#)
- [When a correction for this article is posted](#)

[Click here](#) to choose from all of JBC's e-mail alerts